We are IntechOpen, the world's leading publisher of Open Access books Built by scientists, for scientists

6,900
Open access books available

186,000
International authors and editors

200M
Downloads

154
Countries delivered to

Our authors are among the

TOP 1%
most cited scientists

12.2%
Contributors from top 500 universities

CLARIVATE ANALYTICS
BOOK CITATION INDEX
INDEXED

WEB OF SCIENCE™

Selection of our books indexed in the Book Citation Index
in Web of Science™ Core Collection (BKCI)

Interested in publishing with us?
Contact book.department@intechopen.com

Numbers displayed above are based on latest data collected.
For more information visit www.intechopen.com

Nano-Sized Minerals from Lower Cretaceous Sandstones in Israel Observed by Transmission Electron Microscopy (TEM)

Nurit Taitel-Goldman and Vladimir Ezersky

Abstract

Fine fraction in quartz arenite sandstones from Lower Cretaceous Hatira formation in Israel was observed by Transmission electron microscope (TEM). Samples were collected from Hatira and Ramon craters located in southern part of Israel and from Manara cliff from the northern part of Israel. The additional phases cause yellow, red, dark red and dark violet colors of the layered sandstones. The motivation was to identify the minerals of the fine factions that cause the variations in the colors. The minerals observed were clay minerals, mainly kaolinite ($Al_4Si_4O_{20}(OH)_8$), some illite ($K_{0.65}Al_{2.0}[Al_{0.65}Si_{3.35}O_{10}](OH)_2$) and smectite. Iron oxides were goethite (FeOOH) and hematite (Fe_2O_3), Titanium-iron oxides observed was ilmenite ($FeTiO_3$), and Titanium-oxides were rutile (TiO_2), and anatase (TiO_2). Sulphates observed were jarosite ($KFe_3(SO_4)_2(OH)_6$) and alunite ($KAl_3(SO_4)_2(OH)_6$). Some of the hematite was formed by recrystallization of goethite. Ilmenite disintegrated into small iron oxides mainly hematite. Euhedral to sub-hedral rutile (TiO_2) and anatase (TiO_2) were preserved in clay-minerals. Crystals of alunite and jarosite were observed in sandstones in both craters. They probably crystallized due to some transgression of the Thetis Sea.

Keywords: TEM, sandstones, clay minerals, Fe-oxides, Ti-oxides, sulphates

1. Introduction

During the Lower Cretaceous, siliciclastic sediments were deposited on ter-restial terrestrial partly lacustrine environments [1–3]. The sandstones are quartz (SiO_2) arenite with rounded quartz grains, clay minerals and siltstones. Lower Chemical weathering of the Pan-African continental basement favored silicate weathering, particularly a warm and humid climate, low relief and low sedi-mentation rates which prevailed over large tracts of Gondwana in the aftermath of the Pan-African orogeny [4]. Cretaceous sandstone originates from Paleozoic sandstones, the first-cycle quartz-rich sandstones [5]. The stratigraphic cycles showed progradational – retrogradational trends due to small global sea-level rises which inundated the continent for short periods and fossils were found [6]. In Lebanon similar sandstones were deposited during the Lower Cretaceous [7].

The composition of the sandstones was 85–95% quartz indicating well-sorted sandstone. Sedimentological observations suggest that the Chouf Formation deposited in fluvial, coastal plain and deltaic environments. The origin of the sandstone is from recycling of Paleozoic sandstones. Sandstones of the Lower Cretaceous were deposited and covered by sediments that were deposited after the Thetis Ocean covered the area during the Upper Cretaceous, hence, hard carbonate stones, limestones, dolomites and marls precipitated, overlying the sandstones. At the end of the Mesozoic era, closure of the Thetis Sea yielded formation of the Syrian arc with monoclines of the Hatira and Ramon areas. After regression of the Thetis Sea during the Oligocene, an erosion surface truncated the hard carbonate rocks of the fold's crest and exposed the underlying friable Lower Cretaceous sandstone. For crater (Makhtesh) Hatira, such an erosion base level formed locally and for a limited period in the Early Miocene. The opening of the Ramon crater started in the Early Pliocene, when the Syrian Arc Fold Belt was uplifted and arched and the Dead Sea Rift was established as a deep intercontinental erosion base in the east [8]. In the northern part of Israel, the Lower Cretaceous sandstones were exposed close to the Dead Sea transform fault and uplift of the Manara cliff and formation of Hula valley.

Composition and morphology of the nano-crystals that coat quartz grain reflect the environmental conditions in which they were formed as primary or secondary forms [9].
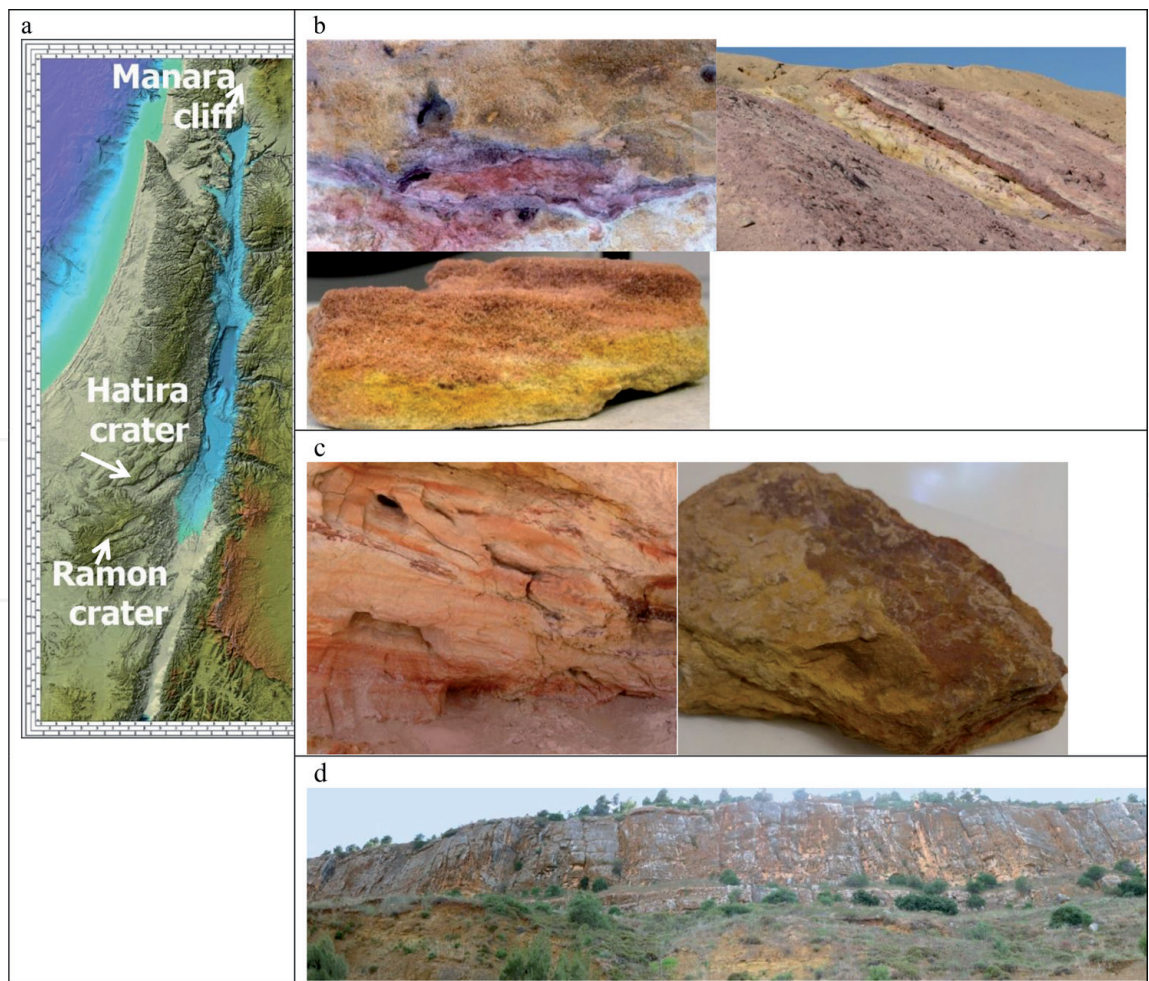

Figure 1.
a. Geomorphological map of Israel. In the northern part is Manara cliff and in the southern part Hatira and Ramon craters. b. Sandstones exposed in the Hatira crater and a sample of red and yellow layers. c. Sandstones exposed in the Ramon crater and a sample with dark violet, red and yellow-red thin layer. d. Sandstones in the Manara cliff.

In this paper, we present Transmission Electron Microscopic (TEM) observation of the nano-sized minerals from Lower Cretaceous sandstones exposed in the Hatira and Ramon craters in southern Israel, and in the Manara cliff in the northern part of Israel (**Figure 1**).

The main motivation of this research is to identify nano-crystals in sandstone that cause the variability in their colors. By using TEM detrital or authigenic phases can be identified.

2. Sampling and methods

The samples that were collected were separated according to their colors: dark violet, violet, dark red, red and yellow (**Table 1**). Sand stone were put for few minutes into an ultrasonic bath, then the fine fraction was separated from the quartz grains and freeze-dried. Each sample was suspended in distilled water and placed on Cu supported holey carbon film and dried. Nano-sized (5–200 nm) particles were checked with Transmission Electron Microscopy (TEM) using a JEOL JEM-2100F analytical TEM operated at 200 kV, equipped with a JED-2300 T Energy Dispersive Spectrometer (EDS) for microprobe elemental analyses. All chemical analyses were obtained by point analyses with a beam width of 1 nm and are presented as atomic ratios. JEOL Analytical Station software, based on the Cliff-Lorimer ratio technique, with an accuracy of ~5%, was used for the calculations. The CuKa line was used to calibrate the spectrometer. Energy-filtered TEM (EFTEM) experiments were performed using a Gatan image filter. The titanium L-edge (456 eV), silicon L-edge (99 eV) and iron L-edge (708 eV) were used for elemental mapping using the three-window method.

No.	Sample	Color	Location	Minerals identified with HRTEM
1	GNH4 YR	Yellow-red	Hatira crater, east	Kaolinite, illite, hematite, goethite
2	GNH4 DR	Dark red	Hatira crater, east	Quartz, clays, jarosite, anatase, goethite, calcite, ilmenite
3	GNH6 R	Red	Hatira crater, east	Kaolinite, ilmenite, hematite, quartz
4	GNR1 V	Violet	Ramon crater northern cliff highway 40	Anatase, kaolinite illite, smectite, goethite, magnetite, maghemite
5	GNR1 Y	Yellow	Ramon crater northern cliff highway 40	Hematite, illite, rutile, quartz
6	GNR2 DV	Dark violet	Ramon crater northern cliff highway 40	Hematite, goethite, kaolinite alunite, apatite
7	GNR2 R	Red	Ramon crater northern cliff highway 40	Goethite, hematite, anatase, illite, kaolinite
8	GNR2 VR	Violet, red	Ramon crater northern cliff highway 40	Hematite, goethite, kaolinite anatase
9	GNR3 R	Red	Ramon crater northern cliff highway 40	Goethite, hematite, kaolinite, illite
10	GNR5 R	Red	Ramon crater northern cliff highway 40	Goethite hematite, anatase, kaolinite, illite, smectite
11	GNKS1	Red	Manara cliff near Kiriat Shmona	Kaolinite, ilmenite, apatite, goethite, quartz

Table 1.
Location, colors and mineral composition in the fine fractions in sandstones from Hatira crater, Ramon crater, and Manara cliff in Israel

Crystalline phases were identified, using Selected Area Electron Diffraction (SAED) in the TEM. With this method, a very high-energy electron beam (200 kV) transmits through the sample and the d-values obtained enabled their identification. The accuracy of the d-values determination was better than 0.005 nm. The smallest area of SAED was 100 nm. If a good lattice image was obtained in very small particles by High Resolution Transmission Electron microscopy, the use of Fast Fourier Transformation (FFT) enabled the identification of the minerals, using the program Digital Micrograph (Gatan).

3. Results

3.1 Hatira crater sandstones

Samples from the Hatira crater were collected at the eastern side of the crater. The colors of the sandstones vary, with thin layers of red sandstone or dark red close to clay layers. Usually the yellow layers are thicker.

In the sample: yellow-red (GNH4 YR), from the Hatira crater (**Figure 2**), a cluster of goethite (FeOOH) with clay minerals, mainly kaolinite ($Al_4Si_4O_{20}(OH)_8$), was observed, and a cluster of hematite (Fe_2O_3) shows the previous morphology of goethite, indicating that hematite was formed by recrystallization of goethite preserving the acicular morphology of goethite. Crystal size of hematite is around 15 nm. Small crystals (25-50 nm) with Ti impurity might reflect ilmenite ($FeTiO_3$) disintegration. The dominance of goethite crystals contributes to the yellow color and hematite contributes to the red color. The recrystallization of goethite into hematite might have happened due to thermal transformation, as the sandstones were covered by younger layers.

Sample GNH4 DR (**Figure 3**) had a dark red color and the minerals identified were clay minerals, small crystals of calcite ($CaCO_3$), jarosite ($KFe_3(SO_4)_2(OH)_6$), goethite, ilmenite, and anatase (TiO_2). The image obtained by TEM shows clay
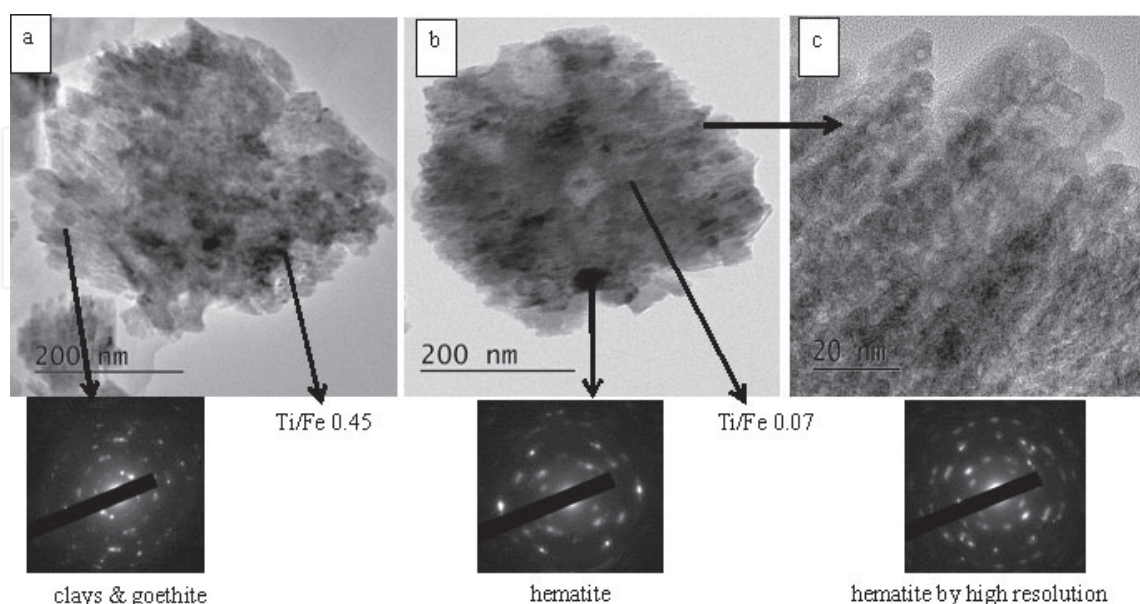

Figure 2.
GNH4 YR images of yellow-red sandstone from the Hatira crater with electron diffractions. Minerals observed were: a. cluster of clay minerals (illite ($K_{0.65}Al_{2.0}[Al_{0.65}Si_{3.35}O_{10}](OH)_2$) and kaolinite, with goethite; electron diffractions of goethite 0.42–0.43 nm in the inner circle. b. Cluster of hematite; electron diffractions of hematite 0.36–0.37 0.268–0.269 nm. c. Tiny crystal of hematite high resolution of hematite formed by recrystallization of goethite preserving the initial phase of goethite. Small crystals had Ti/Fe ratios 0.07 and 0.45. Electron diffractions were 0.36 and 0.27 nm.
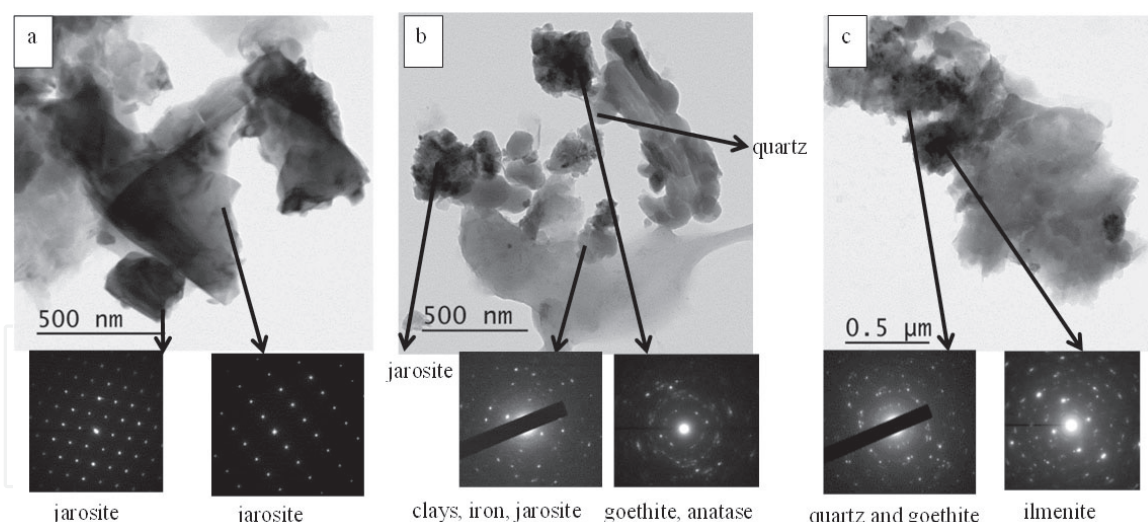
Figure 3.
GNH4 DR dark red sandstone from the Hatira crater. Minerals observed were clay minerals, jarosite goethite, anatase and ilmenite. a. Jarosite with point analyses (%atom) in the lower left side yielded Al-27.28, S-46.69 K-13.91 and Fe-12.12; in the upper part Al-24.38, S-52.13, K-9.32 and Fe-14.17. Electron diffractions at the left side were 0.59 nm, 0.57 nm and 0.28 nm at the central part the electron diffractions were 0.506 nm, 0.3108 nm and 0.3012 nm. b. Minerals observed were clay minerals, jarosite, goethite, anatase with atomic ratio Fe/Ti 0.85. Electron diffractions at the upper part of the images yielded for goethite 0.42 nm and for anatase 0.35. c. Minerals observed were quartz, and ilmenite with electron diffraction of 0.36 nm.

minerals with clusters of anatase and goethite. Jarosite appears with euhedral or sub-hedral morphology, indicating that it was formed in the sandstone. The crystal size of jarosite is 100-200 nm. Ilmenite crystal had Fe/Ti 0.85 and the crystal's size is ≈200 nm.

Sample GNH6 R (**Figure 4**) was collected from a thin red layer and vein within a clay layer in the sandstone. Ilmenite was found as a cluster of small particles surrounded by clay minerals. The ilmenite point analysis had Fe/Ti 0.38, indicating that a larger crystal disintegrated and was preserved within the clay layer. EFTEM RGB color shows disintegration of the ilmenite mineral. Usually ilmenite is resistant to weathering processes and it probably arrived at the area along with the quartz grains. At the lower part of the image hematite formed a layer, causing the red color of the sandstone. Recrystalliztion of ilmenite into hematite was found also in sands along the Mediterranean coast. The precursor and the recrystallized tiny hematite crystals remain close to each other since they are all kept within clay minerals [10].

3.2 Ramon crater sandstones

Sandstones are exposed at the northern cliff of the Ramon crater close to highway 40. Volcanic eruption occurred in the area during the Lower Cretaceous, forming basanite flows and paleosol between the volcanic flows [11]. The samples presented were collected above the basanitic flows. Lower cretaceous sandstones in the Ramon crater have various colors: dark violet, violet, dark red, red and yellow (**Figure 1c**).

The violet sample GNR1V (**Figure 5**) had kaolinite clusters, euhedral crystals of anatase (50-100 nm), magnetite (Fe_3O_4) and maghemite (Fe_3O_4) that was probably formed by magnetite oxidation. Kaolinite crystals had euhedral morphology, indicating that they crystallized in the area. Similar euhedral morphology of some of the anatase and rutile (TiO_2) crystals indicates that they might also have been formed in the sandstone by recrystallization of other phases. Another option is that the euhedral morphology of the Ti-oxides results from their resistance to weathering. In sample GNR1 V, anatase crystals reached a size of 90 nm and Fe/Ti atomic ratios were 0.04–0.26.
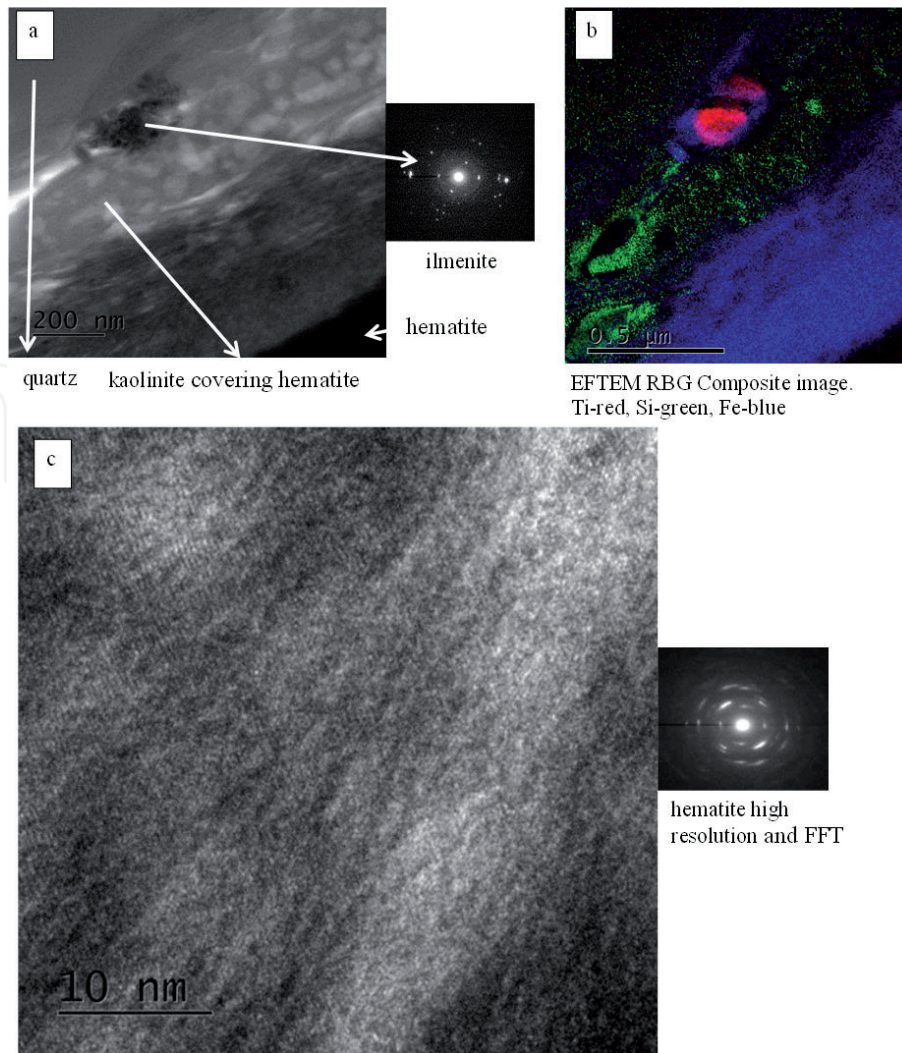
Figure 4.
GNH6 R red sandstone from the Hatira crater: a. cluster of ilmenite with Fe/Ti 0.38 in a kaolinite layer covering hematite layer. The upper gray layer is part of a quartz grain. b. Composition of phases observed on the left side. c. High resolution image of hematite with FFT.

Sample GNR1Y (**Figure 6**) presents additional phases of a yellow sandstone. Quartz grain was observed surrounded by a cluster of illite ($K_{0.65}Al_{2.0}[Al_{0.65}Si_{3.35}O_{10}]$ $(OH)_2$), hematite and a euhedral rutile crystal (250 nm) with Fe/Ti 0.03 atomic ratio. Hematite tiny crystals <100 nm were also observed close to the quartz grain and on the clays.

In sample GNR2 DV dark violet sandstone from the Ramon crater (**Figure 7**), the main clay mineral is kaolinite forming clusters with hematite and alunite ($KAl_3(SO_4)_2(OH)_6$). The largest crystal size of hematite is around 300 nm, contributing to the violet color of the sandstone. Point analysis in % atom of alunite yielded: Al 6.00–6.37, S 2.04–2.34, K 0.29–0.32 and Fe 0.01. Alunite was probably precipitated from acid rain or evaporation of sea water that might have entered the area during the Lower Cretaceous. Tiny crystals of goethite formed clusters with clays.

Sample GNR2 R from red sandstone in the Ramon crater (**Figure 8**) had clay minerals, illite and kaolinite with anatase, goethite and hematite. Anatase (~50 nm) had euhedral morphology, indicating that it might have crystallized in the sandstone. The goethite crystals had acicular morphology (~150 nm); some of the goethite partially recrystallized into hematite preserving the initial acicular goethite morphology. Tiny crystals of hematite were also observed on goethite crystals. A high resolution image was taken from a cluster of hematite preserving outer goethite morphology.
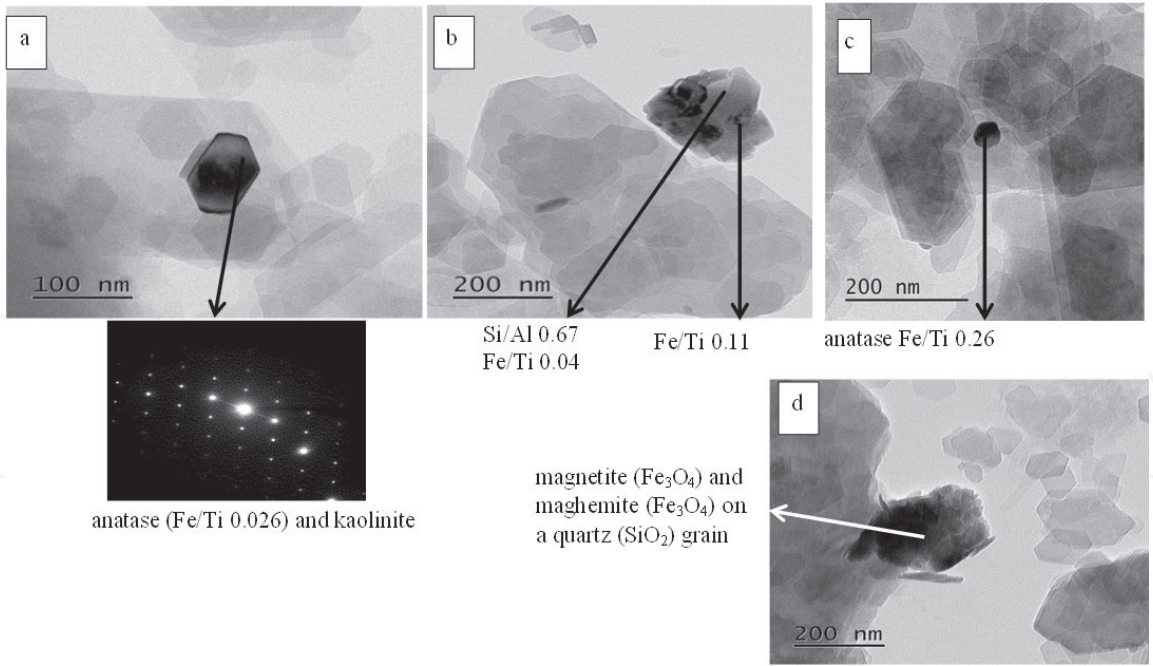
Figure 5.
GNR1 V violet sandstone from Ramon crater. Minerals observed: a, b, c: Anatase with electron diffraction at 0.36 nm and kaolinite. d: Magnetite (Fe_3O_4) and maghemite (Fe_3O_4) on a quartz (SiO_2) grain, kaolinite at the right side.
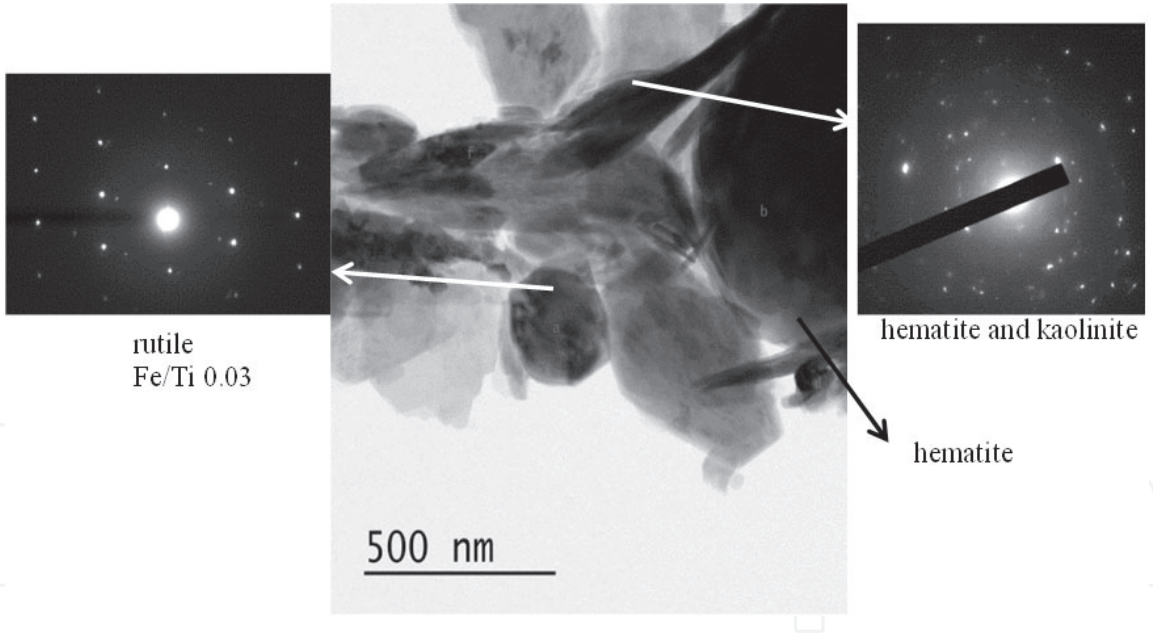

Figure 6.
GNR1 Y. image of yellow sandstone from Ramon crater with electron diffractions. The minerals observed were rutile, hematite illite and kaolinite. Quartz (SiO_2) grain is on the right side.

Sample GNR2 VR (**Figure 9**) is from violet-red sandstone from the Ramon crater. The minerals identified were kaolinite, goethite, hematite and anatase. High resolution of the sample yielded morphology of euhedral acicular crystals that were the initial stage of goethite, and the inner morphology was of small crystals of hematite. Goethite has been transformed into hematite preserving the acicular morphology. The cluster of hematite includes the clay mineral, kaolinite. Euhedral anatase crystal (~60 nm) was observed close to clay minerals with impurity of Fe/Ti 0.027 atomic ratio.
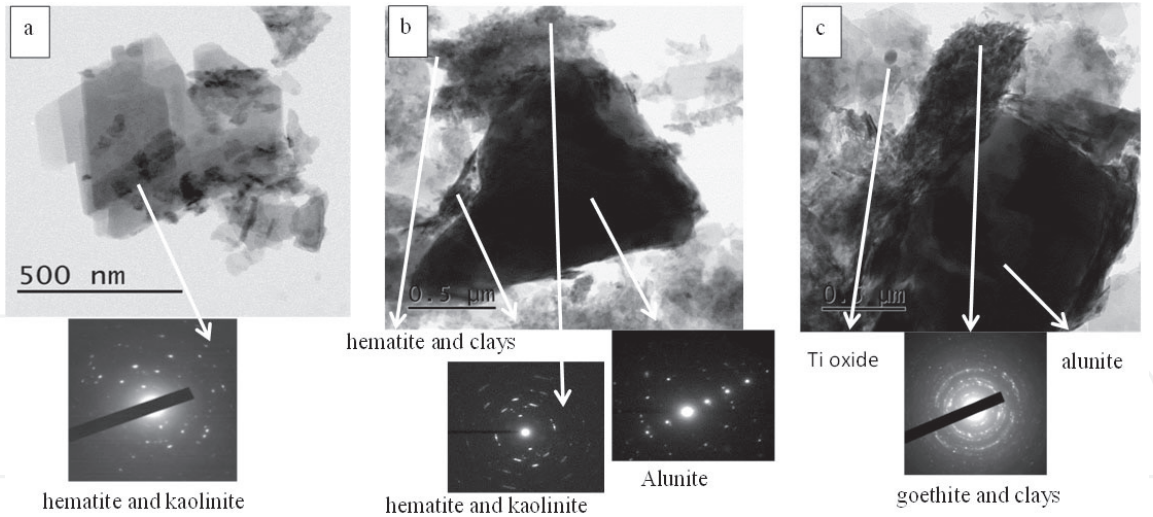
Figure 7.
GNR2 DV image of dark violet sandstone from Ramon crater. Minerals observed were: a. kaolinite and hematite; b. kaolinite, hematite with electron diffraction at 0.37 nm and at the lower part alunite with electron diffraction at 0.5 nm; c. small crystal of Ti-oxide, cluster of goethite with electron diffraction 0.42 nm and alunite crystal on the right side.
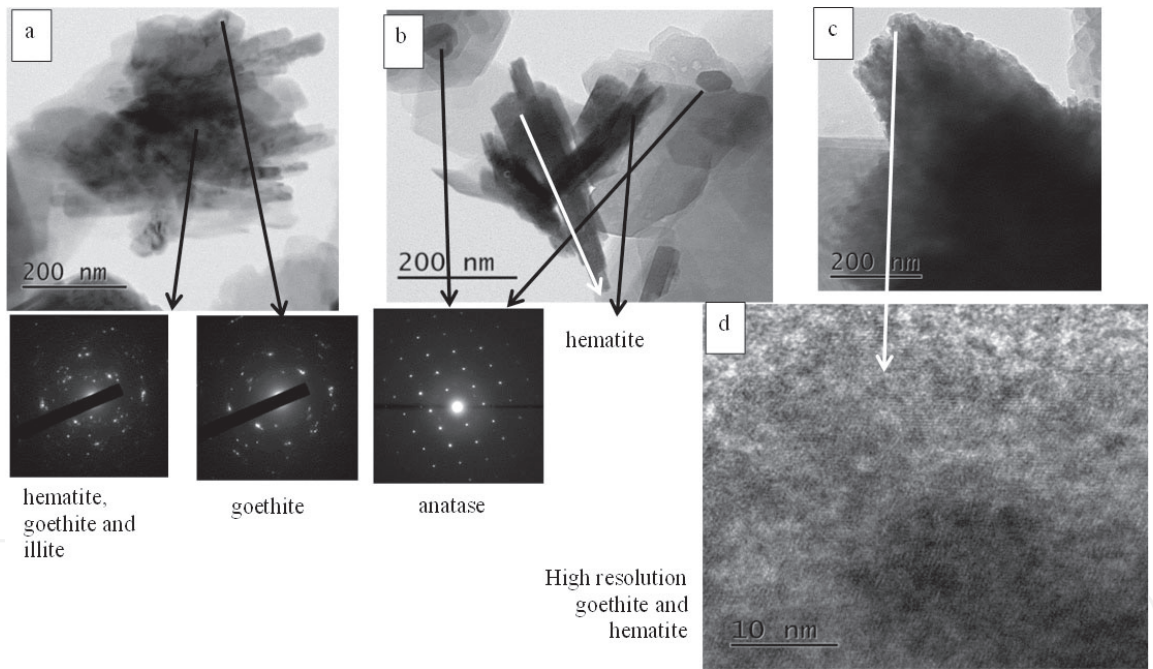

Figure 8.
GNR2 R red sandstone from Ramon crater. Minerals observed: a. goethite and hematite on illite and kaolinite; b. hematite and anatase; c. goethite and tiny crystal of hematite; d. high resolution of goethite and hematite.

Sample GNR3 R (**Figure 10**) red sandstone from the Ramon crater had clusters of goethite with kaolinite, illite and smectite. Small crystals (<50 nm) that were observed on the clays had impurity of Ti with the atomic ratio of Ti/Fe 0.027. These crystals might result from disintegration of ilmenite.

Sample GNR5 R (**Figure 11**) red sandstone from the Ramon crater had clay minerals, goethite crystals and anatase (TiO_2). The size of the goethite crystals reached 800 nm.The size of euhedral anatase crystal was 200 nm and impurity of iron was Fe/Ti 0.04 atomic ratio. From a dark field image obtained, tiny crystals of anatase are located in the upper part of the image.
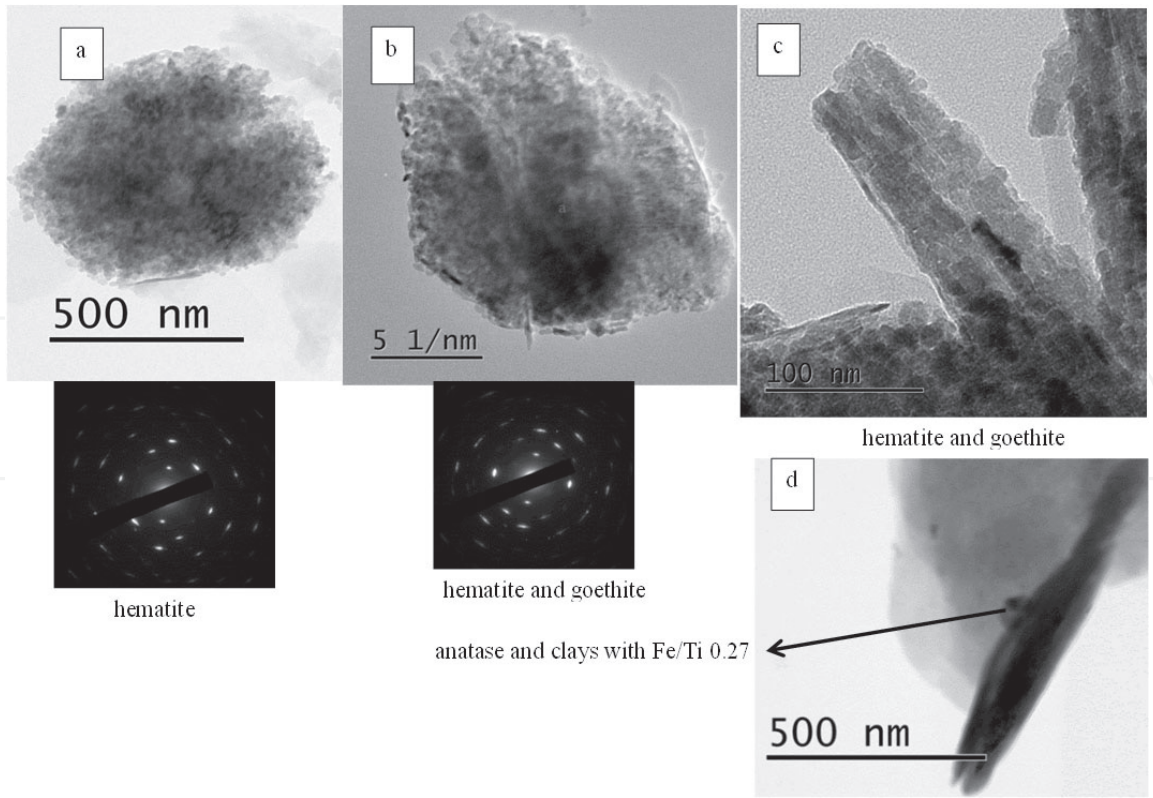
Figure 9.
GNR2 VR violet-red sandstone from Ramon crater. Minerals observed: a. a cluster of hematite with electron diffraction 0.367–0.374 nm; b. hematite electron diffraction 0.367–0.377 nm and goethite electron diffraction 0.42 nm; c. high resolution of hematite preserving initial crystals of goethite electron diffractions 0.365–0.375 nm; d. anatase (TiO₂) with iron impurity and clays.
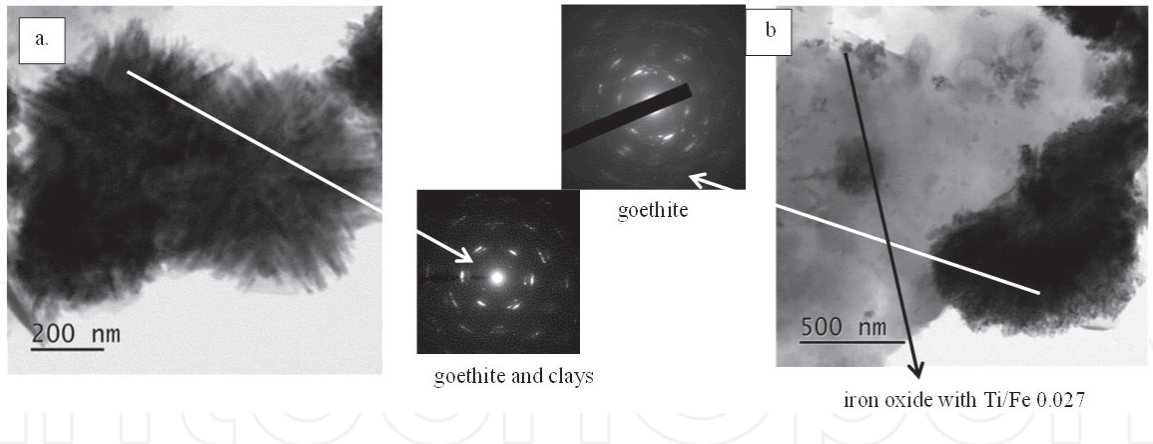

Figure 10.
GNR3 R red sandstone from Ramon crater: a. Kaolinite, smectite and illite with electron diffractions of 0.45nm and goethite. b. Lay minerals and goethite electron diffraction 0.41 nm.

3.3 Sandstone on Manara cliff

Sandstones of Lower Cretaceous were exposed in the northern part of Israel due to uplift along the Dead Sea transform fault. The main phases identified in the fine fraction were clay minerals, mainly kaolinite, ilmenite and hematite (**Figure 12**). The size of ilmenite crystals varies between 1000 nm and 50 nm. Most of the ilmenite crystals disintegrate into small crystals and Fe/Ti ratios decrease. The tiny ilmenite crystals are preserved in clays covering a quartz grain. Hematite tiny crystals that result from disintegration of ilmenite and recrystallize into hematite are preserved within clay minerals.
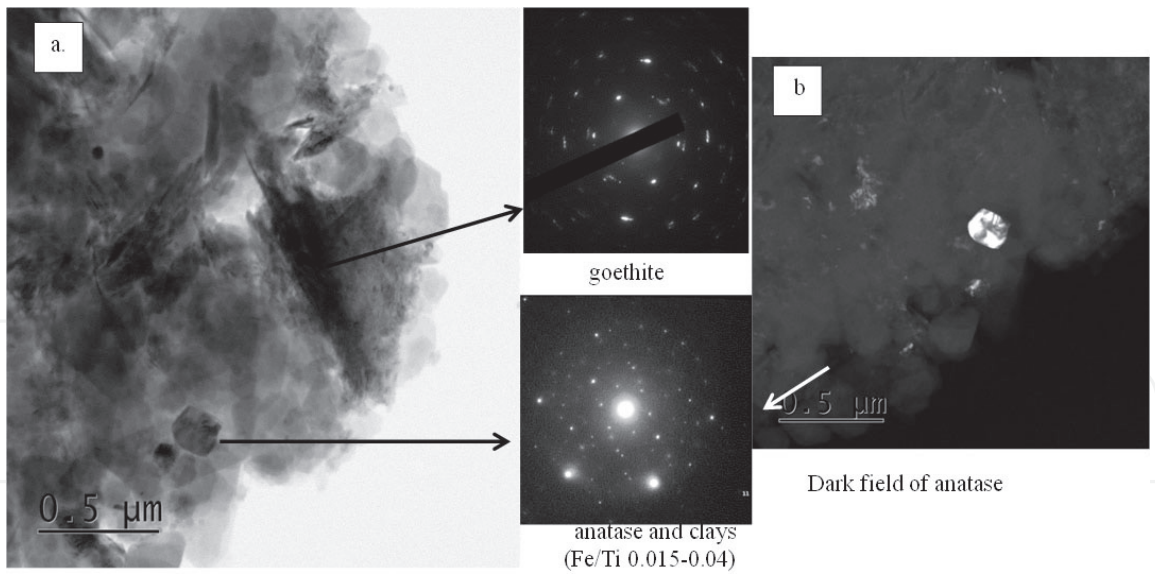
Figure 11.
GNR5 R red sandstone from Ramon crater. a. Minerals observed with electron diffraction were: anatase and goethite surrounded by clays. b. Dark field image showing larger anatase crystal and small crystals of anatase in the area.
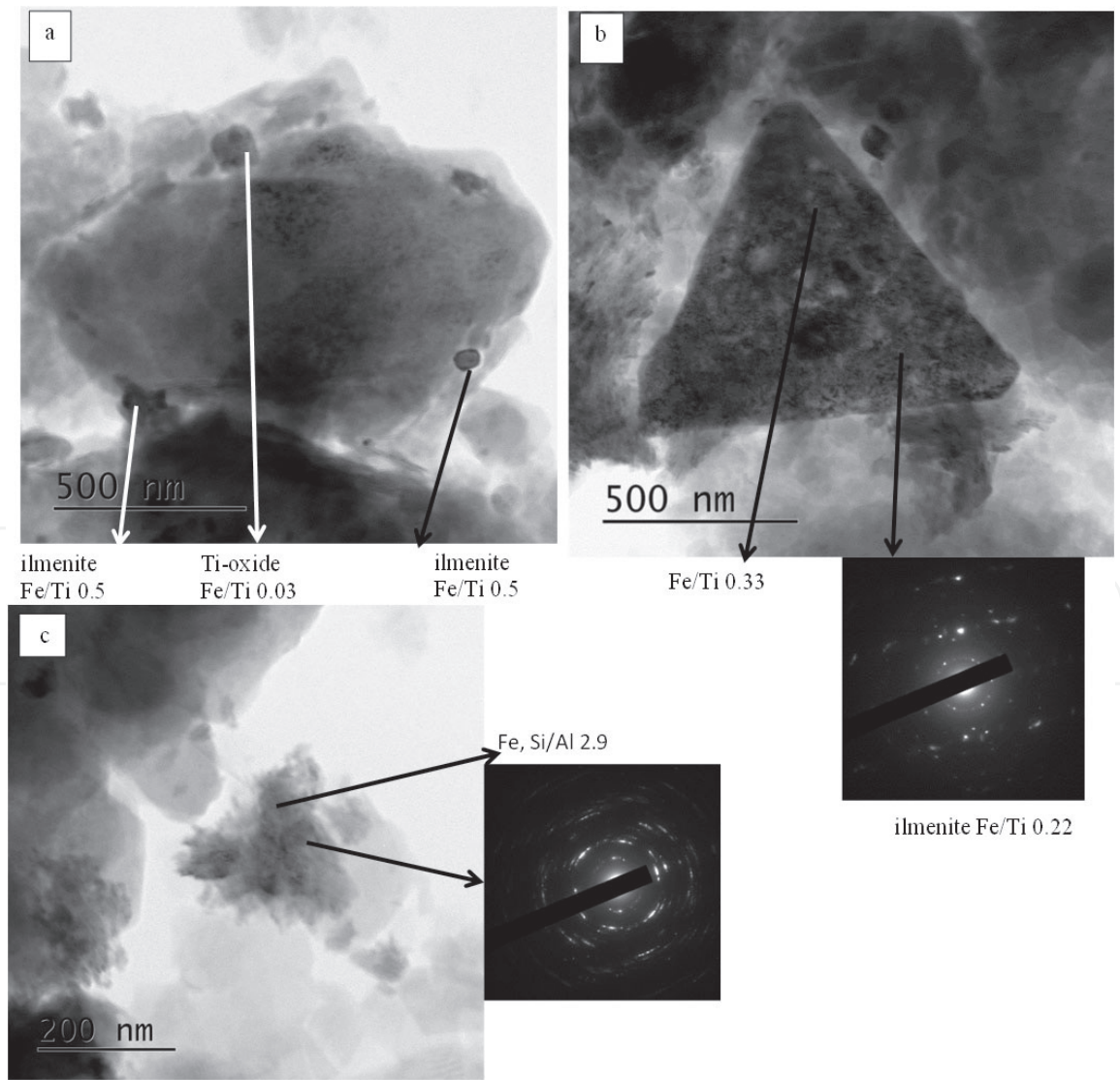

Figure 12.
GNKS1 sandstones exposed in Manara cliff. Minerals observed: a. clays and ilmenite; b. ilmenite electron diffraction 0.255 nm; c. cluster of hematite with electron diffraction of 0.37–0.38 nm and clays over a small quartz (SiO_2) grain on the upper left side quartz grain and clays.

4. Discussion

The Lower Cretaceous sandstones are mainly quartz arenite with rounded quartz grains that were separated from the fine fraction. These sandstones originated from Paleozoic sandstones that were the first-cycle quartz-rich sandstones and resulted from widespread chemical weathering of the Pan-African continental basement [4]. The composition of the sandstones changes from the arkose at the lower layers to sub-arkose and the younger layers are mainly mature quartz arenite [12, 13]. The fine fraction includes minerals that were formed by disintegration of the initial phases or result from dust storms.

Clay minerals usually cover the quartz grains. In the samples studied the dominant clay mineral is mainly kaolinite, small amounts of illite and some smectite. Kaolinite is usually crystallized at permeable bedrock in warm, moist regions forming as a residual weathering product. Illite might result from weathering of muscovite or K-feldspar [14], and smectite was formed from weathering of other minerals like biotite or amphibole that were in the Paleozoic sandstones from the first cycle. The crystal size of kaolinite is around 200-500 nm. Quartz-arenite stones from the Lower Miocene Moghra in Egypt were studied showing similar results with smectite, illite and kaolinite as clay minerals and hematite as the iron oxide [15].

Iron oxides were goethite, hematite, and some magnetite and maghemite. The iron oxides are responsible for the colors of the sandstones. Similar results were found in sands on the Atlantic coastal plain as iron oxides coat sand grains [16]. Goethite is usually yellow but impurities might change its color. Crystal's size might also affect the color. Goethite crystal sizes of 300 nm–1000 nm cause a yellow color; with smaller crystals it becomes darker. Hematite is usually yellow-red but larger crystals cause the appearance of a purple color. Formation of the iron oxides depends on the environment in which they were crystalized. Goethite usually crystallizes at fast oxidation at lower pH [17]. Hematite results from recrystallization of goethite close to a clay layer that adsorbs the OH of goethite, and hematite crystallizes (**Figure 2a**). Hematite and ilmenite ($FeTiO_3$) form a solid solution. Disintegration of ilmenite formed hematite crystals with Ti impurity and the leftover of the ilmenite was enriched with Ti forming Fe/Ti < 1 ratios.

Rutile (TiO_2) and anatase (TiO_2) had euhedral morphology, indicating that they might have crystallized in the area or, due to their hardness, they preserved their initial morphology. Rutile was found in the Paleozoic sandstone along with tourmaline [18]. Fe impurity in Ti-oxides might indicate that they were formed by in the area as ilmenite disintegrated and they were preserved within the surrounding clay minerals. It is also possible that rutile and anatase recrystallized from biotite from the magmatic and metamorphic rocks from the basement [19].

Jarosite ($KFe_3(SO_4)_2(OH)_6$) and alunite ($KAl_3(SO_4)_2(OH)_6$) were observed in dark violet or dark red sandstones. Jarosite was found in younger marl layers of Taqiya formation in the southern part of Israel, as a result of alteration of pyrite [20]. It was also found in Jurassic sandstone in the Ramon crater, and two possible formation processes were suggested: acid rain or from transgression, for a short period, of the sea [21]. Usually jarosite and alunite form a solid solution and they crystalize in saline lakes or acid sulphate soils [22]. In Utah (USA) they form cement in Jurassic sandstones and they precipitated in marginal marine to coastal dune [23]. Jarosite usually formed at low pH conditions and it requires an arid environment to prevent its decomposition into ferric oxyhydroxides [24]. It is possible that both jarosite and alunite were crystallized due to short transgression episodes of the Thetis Sea.

5. Conclusions

Quartz arenite sandstones were formed during Lower Cretaceous in the southern and northern parts of Israel. The fine fraction observed by TEM includes clay minerals mainly kaolinite and small amounts of illite and smectite. Additional minerals that contribute to the colors of the sandstones are iron oxides, goethite and hematite. The initial phase of iron oxides that coat quartz grains or form clusters was goethite, and hematite crystals preserved the initial acicular goethite structure. Ilmenite preserved within clay minerals disintegrate into small crystals enriched with iron. The tiny euhedral crystals of Ti oxides were probably formed in the sand. Jarosite and alunite observed in Ramon and Hatira craters were crystallized in the sandstones due to short transgression of the Thetis Sea.

Acknowledgements

Author details

Nurit Taitel-Goldman[1*] and Vladimir Ezersky[2]

1 The Open University, Raanana, Israel

2 Ilse Katz Institute for Nanoscale Science and Technology, Ben-Gurion University of the Negev, Beer-Sheva, Israel

*Address all correspondence to: nurittg@hotmail.com

IntechOpen

References

[1] Bentor Y.K. and Vroman A., 1960, The geological map of Israel on a 1:100000 scale. Series A – The NegeV Sheet 16: mount Sdom (with explanary text) *Geol. Surv. Isr.*, 117p.

[2] Frank R. and Benjamini C., 2017, Field excursion in the Hatira anticline, northern Negev: High resolution sequence stratigraphy of the Aptian-Albian Hatira Succession. *Field trip guides Israel geological society, Mitzpe Ramon*, e1-e33.

[3] Lewy Z., 2003, Lower Aptian trace fossils in marginally marine sandstone and their extant analogues. *Isr. J. Earth Scie*. 52 39-46.

[4] Avigad D., Sandler A., Kolodner K., Stern R.J., McWilliamsM., Miller N. and Beyth. M., 2005, Mass-production of Cambro–Ordovician quartz-rich sandstone as a consequence of chemical weathering of Pan-African terranes: Environmental implications. *Earth and Planetary Science Letters.* 240 818-826.

[5] Kolodner K., Avigad D., Russel Ireland T. and Garfunkel Z., 2009, Origin of Lower Cretaceous ('Nubian') sandstones of North-east Africa and Arabia from detrital zircon U-Pb SHRIMP dating. Sedimentology 56 2010-2013.

[6] Wiessbrod T., 2002, stratigraphy and correlation of the lower Cretaceous exposures across the Dead Sea Transform with emphasis on tracing the Amir formation in Jordan. *Isr. J. Earth Sci*. 51 55-78.

[7] Tari G. et al. (2020) The Lower Cretaceous Chouf Sandstone of Lebanon: A Regional Reservoir Level in the Levant?. In: Khomsi S., Roure F., Al Garni M., Amin A. (eds) Arabian Plate and Surroundings: Geology, Sedimentary Basins and Georesources. Regional Geology Reviews. Springer,

Cham. https://doi-org.elib.openu.ac.il/10.1007/978-3-030-21874-4_2

[8] Zilberman E., 2000, Formation of "makhteshim" - Unique erosion cirques in the Negev, southern Israel. Isr. J. Earth Sci. 49 3 127-141.

[9] Schindler M. and Singer D.M., 2017, Mineral surface coatings: environmental records at the nanoscale. Elements 13 159-164.

[10] Taitel-Goldman N., 2013, Recrystallization processes involving iron oxides in natural environments and In vitro, in: P. Wilson (editor) *Recent developments in the study of recrystallization.* InTech - open science - open minds, Rijeka, Croatia ISBN 978-953-51-0962-4

[11] Singer A., 1975, A Cretaceous laterite in the Negev Desert, Southern Israel. Geological magazine 112 151-162.

[12] Weissbrod, T., 1980, The Paleozoic of Israel and adjacent countries (a lithostratigraphic study): *(Ph.D. thesis) Jerusalem*, *Israel, Hebrew University of Jerusalem*, 255pp.

[13] Weissbrod, T. Perath I., 1990, Criteria for the recognition and correlation of sandstone units in the Precambrian and Paleozoic-Mesozoic clastic sequence in the Near East. *J. Afr. Earth Sci*. 10 253-270.

[14] Shelukhina O., El-Ghali M., AbbasiI.A., Hersi O.S. Farfour M., Ali A., Al-AwahH., Siddiqui N. A., 2021, Origin and control of grain-coating clays on the development of quartz overgrowths: example from the lower Paleozoic Barik Formation sandstones, Huqf region, Oman, 2021, Arab J Geosci. 14, 210.

[15] Tawfik H.A., Salah M.K. , Maejima W., Armstrong-Altrin J.S.,

Abdel-Monem T., A.H., El Ghandour M.M., 2018, Petrography and geochemistry of the Lower Miocene Moghra sandstones, Qattara Depression, north Western Desert, Egypt, *Geological journal* 53 1938-1953.

[16] Penn RL., Zhu C., Xu H., Veblen DR., 2001, Iron oxide coatings on sand grains from the Atlantic coastal plain. High resolution Transmission electron microscopy characterization. Geology 29 843-846.

[17] Cornell, R.M. and Schwertmann U., 2003, The Iron oxides, structure, properties, reactions, occurrences and uses. *Wiley-VCH verlagGmbH&Co. KGaA, Wieinheim.*

[18] Weissbrod, T., Nachmias J., 1987, Stratigraphic significance of heavy minerals in the Late Precambrian-Mesozoic clastic sequence (Nubian Sandstone) in the near east. Sediment. Geol. 47 263-291.

[19] Morad S. and Aldahan A., 1982, Authogenesis of titanium minerals in two Proterozoic sedimentary rocks from southern and central Sweden. *Journal of sedimentary petrology* 52. 4, 1295-1305.

[20] Sass E., Nathan Y., Nissenbaum A., 1965, Mineralogy of certain pyrite concretions from Israel and their alteration products. *Mineralog.* Mag, 35 84-87.

[21] Goldbery R., 1978, Early diagenetic nonhydrothermal Na-alunite in Jurassic flint clays, Makhtesh Ramon. Israel. Geol. Soc.Am. bull. 89 687-698.

[22] Jones F., 2017, Crystallization of Jarosite with variable Al^{3+} content: the transition to Alunite. MDPI Minerals 7 90.

[23] Potter-McIntyre S.L. and McCollom T.M., 2018, Jarosite and Alunite in ancient terrestrial sedimentary rocks: reinterpreting Martian depositional and diagenetic environmental conditions. MDPI Life 8 32.

[24] Bell J. H., Beitler Bowen, Martini, 2010, Imaging spectroscopy of jarosite cement in the Jurassic Navajo Sandstone. Remote Sensing of Environment 114 2259-2270.